Kinetics and Interactions of Molybdenum and Iron−Sulfur Centers in Bacterial Enzymes of the Xanthine Oxidase Family: Mechanistic Implications

Christoph Canne,[‡] David J. Lowe,[§] Susanne Fetzner,[||] Benjamin Adams,[⊥] Andrew T. Smith,[⊥] Reinhard Kappl,[‡] Robert C. Bray,[#] and Jürgen Hüttermann*[,‡]

Fachrichtung Biophysik und Physikalische Grundlagen der Medizin, Universität des Saarlandes, Klinikum Geb. 76, D-66421 Homburg/Saar, Germany, John Innes Centre, Colney, Norwich NR4 7UH, U.K., School of Biological Science, University of Sussex, Brighton BN1 9QG, Sussex, U.K., School of Chemistry, Physics and Environmental Science, University of Sussex, Brighton BN1 9QJ, Sussex, U.K., and Fachbereich Biologie, Carl von Ossietzky Universität Oldenburg, Postfach 2503, D-26111 Oldenburg, Germany

Received May 12, 1999; Revised Manuscript Received August 16, 1999

ABSTRACT: For isoquinoline 1-oxidoreductase (IsoOr), the reaction mechanism under turnover conditions was studied by EPR spectroscopy using rapid-freeze methods. IsoOr displays several EPR-active Mo(V) species including the "very rapid" component found also in xanthine oxidase (XanOx). For IsoOr, unlike XanOx or quinoline 2-oxidoreductase (QuinOr), this species is stable for about 1 h in the absence of an oxidizing substrate [Canne, C., Stephan, I., Finsterbusch, J., Lingens, F., Kappl, R., Fetzner, S., and Hüttermann, J. (1997) *Biochemistry 36,* 9780−9790]. Under rapid-freeze conditions in the presence of ferricyanide the very rapid species behaves as a kinetically competent intermediate present only during steady-state turnover. To explain the persistence of the very rapid species in IsoOr in the absence of an added oxidant, extremely slow product dissociation is required. This new finding that oxidative conditions facilitate decay of the very rapid signal for IsoOr supports the mechanism of substrate turnover proposed by Lowe, Richards, and Bray [Lowe, D. J., Richards, R. L., and Bray, R. C. (1997) *Biochem. Soc. Trans. 25,* 774−778]. Additional stopped-flow data reveal that alternative catalytic cycles occur in IsoOr and show that the product dissociates after transfer of a single oxidizing equivalent from ferricyanide. In rapid-freeze measurements magnetic interactions of the very rapid Mo(V) species and the iron−sulfur center FeSI of IsoOr and QuinOr were observed, proving that FeSI is located close to the molybdopterin cofactor in the two proteins. This finding is used to relate the two different iron−sulfur centers of the aldehyde oxidoreductase structure with the EPR-detectable FeS species of the enzymes.

Molybdenum containing enzymes can be found in many organisms and are involved in numerous biological transformations (*1*−*11*). On the basis of the structure of the molybdenum cofactor, these enzymes can be categorized into three subgroups (*11*): the sulfite oxidase family, the dimethyl sulfoxide reductase group, and the xanthine oxidase family. Recently, crystal structures of some members of these groups have been determined. In the xanthine oxidase group, the crystal structure of aldehyde oxidoreductase from *Desulfovibrio gigas* was resolved (*12*, *13*), revealing the spatial relationships of the molybdopterin center and the two [2Fe-2S] clusters, one of which is hydrogen bonded to the pterin cofactor. Xanthine oxidase itself (XanOx)[1] contains, in addition, a flavin adenine dinucleotide.

In recent work, we have described in detail the EPR characteristics and redox potentials of redox active centers from quinoline 2-oxidoreductase (QuinOr), isoquinoline 1-oxidoreductase (IsoOr), and quinaldine 4-oxidase (QualOx), three bacterial members of the xanthine oxidase family (*14*, *15*). Among these three enzymes, the molybdenum signals of QuinOr and QualOx show close similarities to those of XanOx, whereas the non-flavin-containing protein IsoOr shows remarkable discrepancies concerning the so-called "very rapid" signal. This signal denoted "very rapid i" in IsoOr, which in XanOx is attributed to the Mo(V) complex formed in the intraenzymatic reoxidation process of the molybdenum center, turns out to be stable for more than 1 h at 20−25 °C in the absence of an oxidizing substrate. In contrast, the very rapid signal of XanOx behaves as a transient in the presence or absence of the oxidizing substrate with a much shorter life span (10 ms in the case of using xanthine as substrate and 1 s in the case of 2-oxo-6-

[†] This work was supported by grants from the Deutsche Forschungsgemeinschaft (DFG), grants Hu 248/11-2 and Fe 383/4-2. Work at University of Sussex was supported in part by a grant from the Wellcome Trust.

* To whom correspondence should be addressed.
[‡] Universität des Saarlandes.
[§] John Innes Centre, Norwich.
[||] Universität Oldenburg.
[⊥] Biological Sciences, University of Sussex.
[#] Chemistry, Physics and Environmental Science, University of Sussex.

[1] Abbreviations: EPR, electron paramagnetic resonance; IsoOr, isoquinoline 1-oxidoreductase; XanOx, xanthine oxidase; QuinOr, quinoline 2-oxidoreductase; QualOx, quinaldine 4-oxidase; FeSI, less anisotropic iron-sulfur-center; FeSII, more anisotropic iron−sulfur-center; FAD, flavin adenine dinucleotide; Tris−HCl, Tris(hydroxymethyl)aminomethane hydrochloride; Ches, 2-cyclohexylamino-ethansulfonic acid.

10.1021/bi991089s CCC: $18.00 © 1999 American Chemical Society
Published on Web 10/01/1999

methylpurine at 20−25 °C) (*3*, *16*). In addition to the very rapid i species, a so-called "rapid i" signal can be observed in IsoOr, which arises shortly after substrate addition, but vanishes within a time scale of approximately 10 min at room temperature.

To clarify the role of the very rapid i signal in IsoOr, further studies in the fast time regime and in the presence of potassium ferricyanide, an artificial substitute of the unknown physiological electron acceptor, were conducted. In this paper, we present results of rapid-freeze studies combined with EPR and supplemented by optical stopped-flow experiments, elucidating the mechanism of action of the enzyme IsoOr. These results will be discussed with respect to the two models of the reaction mechanism of xanthine oxidase that have been described. The first one implies a nucleophilic attack on C-8 of the substrate xanthine by a deprotonated water ligand of the molybdenum center (*11*, *17*). The mechanism of Lowe, Richards, and Bray postulates a side-bonded Mo−C═O structure of the very rapid species, generated by addition of the xanthine C-8-H bond across the Mo═S bond with subsequent attack of the resulting intermediate by the deprotonated water ligand (*18*).

One important advantage of EPR spectroscopy is its ability to resolve magnetic interactions between neighboring paramagnetic centers. We have thoroughly analyzed interactions between both reduced iron−sulfur centers and between the molybdopterin cofactor and the iron−sulfur centers. We use our results to address the question of which one of the iron−sulfur EPR signals should be attributed to the center lying close to the molybdenum cofactor in the structure of aldehyde oxidoreductase.

MATERIALS AND METHODS

Preparation of Enzyme Samples. Samples of the enzymes QuinOr, IsoOr, and QualOx were prepared as described in previous publications (*14*, *19*, *20*). IsoOr subunit concentrations were estimated from $\epsilon_{450nm} = 21.3\ mM^{-1}\ cm^{-1}$. The sample of this enzyme used for rapid-freeze and stopped-flow experiments was assumed (see Results) to be 80% functional, and concentrations of functional enzyme were based on correction by this factor. The activity of IsoOr was assayed by following the reduction of the artificial electron acceptor potassium ferricyanide (1 mM) at 420 nm, with isoquinoline (0.5 mM), at pH 10.0 in 250 mM Na^+-Ches at 21 °C.

Preparation of EPR Samples. Samples generated by manual freezing were prepared as reported previously (*15*). Solutions of 5 mM of the substrate isoquinoline in 2-propanol or ethanol were added to 45 μM IsoOr samples, transferred into quartz tubes and frozen in liquid nitrogen within 1 min. Samples reduced with dithionite for comparison were incubated under a nitrogen atmosphere for about 5 min after addition of the reducing agent and frozen in liquid nitrogen. The desulfo-form of QuinOr was prepared by reaction of native QuinOr with potassium cyanide and subsequent reduction with dithionite. Samples were prepared by rapid freezing (*21*) using the equipment described in ref *22*.

EPR Spectroscopy. EPR spectra at X-band frequencies were recorded on a Bruker ESP 300 spectrometer equipped with a continuous flow helium cryostat (ESR 900, Oxford Instruments) for the temperature range 5−80 K. The magnetic field and the microwave frequency were determined with an NMR gaussmeter and a microwave counter, respectively. The modulation amplitude for spectra recording generally was 0.5 mT. Absolute signal intensities were determined by double integration using Cu^{2+}−EDTA as standard and correcting for isopentane in the rapid-freeze samples, for ^{95,97}Mo hyperfine lines not included and for transition probability (*23*). For simulation of the Mo(V) spectra and their interaction with iron−sulfur signals, the program *Win-EPR Simfonia*, Version 1.25 from Bruker Instruments was used. The dipolar magnetic interaction between adjacent paramagnetic centers was modeled by the term $S_1 \cdot \mathbf{D} \cdot S_2$, with S_1 and S_2 being the spin of the individual centers. It causes a zero-field splitting (zfs) for both centers, which is described by the axial splitting parameter D and a rhombic zfs parameter *E*. The zfs term *D* is proportional to r^{-3} (*r* distance between the two interacting centers).

Stopped-Flow Experiments. An Applied Photophysics SX.18 MV stopped-flow apparatus operated in single wavelength mode was used. Data were analyzed with the help of the maker's software ("Pro-K"); iterative fitting to the differential equations corresponding to Scheme 3 was performed using a FORTRAN program based on NAG Library routines E04JBF, which is a quasi-Newton algorithm for finding a minimum of a function, and D02BAF, which integrates a system of first-order ordinary differential equations over an interval using a Runge−Kutta−Merson method.

RESULTS

EPR Measurements. Figure 1 shows EPR spectra obtained from IsoOr under rapid-freeze conditions and measured at 80 and 30 K, respectively. The enzyme was allowed to react with a small excess of the substrate isoquinoline in the presence of excess ferricyanide under aerobic conditions at pH 10. As in the "manual freeze" samples without ferricyanide (*15*), a highly anisotropic signal appeared at 80 K in the time scale up to 220 ms (Figure 1, spectrum a, 9 ms), which could be identified as the very rapid i (i for IsoOr) signal with $\mathbf{g}_1 = 2.024$, $\mathbf{g}_2 = 1.955$, $\mathbf{g}_3 = 1.941$. After 2 s, the signal vanished (spectrum b). Obviously, the artificial electron acceptor ferricyanide has reduced the lifetime of the very rapid i signal efficiently. The rapid-freeze sample obtained after 9 ms reaction time yielded spectrum c when recorded at 30 K. The very rapid i signal (denoted VR) now shows a doublet splitting of approximately 0.7 mT at $\mathbf{g}_2$ marked by the stick diagram, whereas only a broadening of the $\mathbf{g}_1$-component of about 0.3 mT is noted. Its $\mathbf{g}_3$-line is hidden under the $\mathbf{g}_2$-component of the more prominent signal from the iron sulfur cluster FeSI, the lines of which are denoted I_i ($i = 1$, 2, and 3 for the respective **g**-factors) in Figure 1c. The typical resonance peaks of the more rhombic iron sulfur center FeSII (marked II_i in Figure 1c) center are hardly developed. At this temperature, samples when fully reduced with dithionite usually contain this FeSII species and a dipolar interaction between the two FeS-centers induces a splitting of the FeSI signal (I_{1a}, I_{1b}) as can be inferred from spectrum e (*15*). The absence of the splitting of FeSI in trace c additionally confirms that only small amounts of the FeSII center are present in the rapid-freeze sample. Hence, the two electrons transferred from the substrate are mainly distributed on molybdenum and FeSI. These centers interact magnetically, giving rise to the splitting of the very rapid i signal.

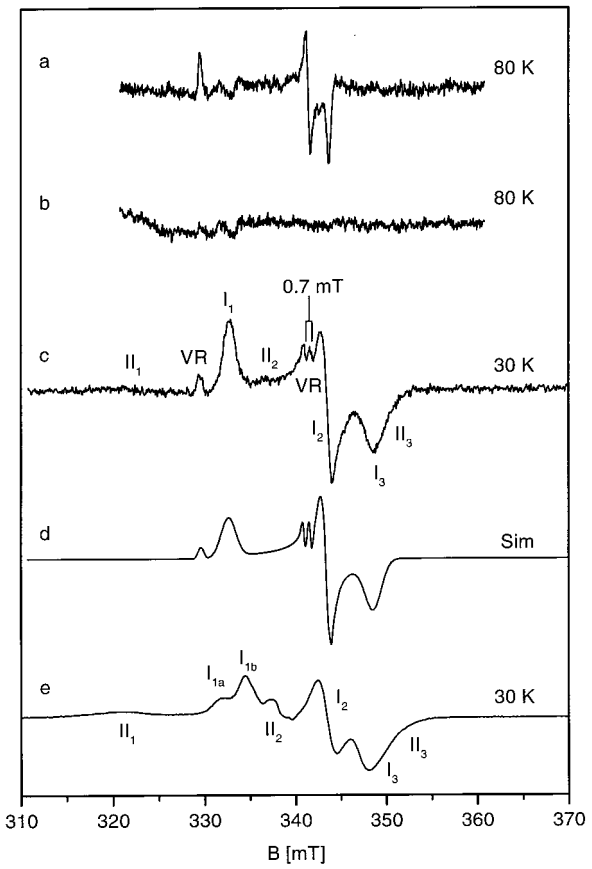

FIGURE 1: (a-c) Rapid-freeze EPR spectra of IsoOr (18 μM functional enzyme) from *Pseudomonas diminuta* 7 after reaction with isoquinoline (45 μM) and potassium ferricyanide (1 mM) in Ches buffer. (a) Spectrum after 9 ms, (b) after 2 s reaction time with only traces of very rapid i left. (c) Spectrum obtained after 9 ms reaction time showing the presence of very rapid i, FeSI and only traces of FeSII. The $\mathbf{g}_1$ component of FeSI lacks the splitting associated to the dipolar coupling with reduced FeS centers (see trace e), the $\mathbf{g}_2$ component of the very rapid i species shows a magnetic interaction with FeSI of approximately 0.7 mT (indicated by sticks). Trace (d) shows a simulation of spectrum (c) with the parameters given in Table 1 and with the relative intensities of the signals adjusted to reflect saturation of the Mo(V) signal. (e) EPR spectrum (30 K) of a dithionite reduced IsoOr sample showing the splitting of the $\mathbf{g}_1$ component of FeSI. Spectra a and b were recorded at 80 K, c and e at 30 K, the modulation amplitude was 0.5 mT (VR, molybdenum very rapid i; I, FeSI center; II, FeSII center).

Figure 1d presents a simulation of the FeSI and the very rapid i signal including the magnetic interaction between them. The parameters of the simulation are given in Table 1. The **g**-factors of FeSI and very rapid i were taken from our previous publication (*15*), the interaction was simulated by introducing an anisotropic **D** tensor, which has a maximal component of 0.7 mT along $\mathbf{g}_2$. For simulation, it was assumed that the principal axes of the electron Zeeman and zero field interactions coincide. The **D** tensor was applied to both interacting species. For FeSI, however, the intrinsic line width is so high that the observed line width is not visibly affected by the splitting pattern.

In Figure 2 the rapid-freeze spectra with (a and c) or without (b and d, respectively) addition of ferricyanide are compared at the respective temperatures of 80 and 30 K. In the samples without the artificial electron acceptor ferricyanide, the features described above are also observable, i.e., at 10 ms the very rapid i species has already developed and, of the FeS centers, FeSI is almost exclusively present, with an unsplit $\mathbf{g}_1$ component. When excess substrate concentrations were used as in the manual freeze measurements (*15*), the same spectral features were observed. One therefore has to conclude that up to 10 ms the enzymatic time course is independent of the presence or absence of an electron acceptor or the substrate concentration.

To gain more information about the magnetic interaction of the molybdenum very rapid i species with FeSI, the IsoOr samples incubated with an excess concentration of 2.5 mM isoquinoline were examined under manual freeze conditions. In Figure 3, the spectra obtained after approximately 4 min of reaction time are displayed. Apart from the reaction time, the only difference in the experimental conditions compared with the rapid-freeze spectra of Figure 2 is the choice of buffer. It was found that the spectra obtained at pH 8 (Tris-HCl) give a much higher signal intensity of very rapid i than the spectra obtained with Ches buffer at pH 10 (compare traces a and b). Therefore, the pH 8-Tris buffer was preferred. Two differences between these spectra and the rapid-freeze results (Figures 1 and 2) are striking. First, the rapid signal (marked R) of IsoOr can now be measured at 80 K. Furthermore, the spectra at lower temperatures than 80 K show that FeSII centers are formed in significant concentrations (Figure 3c). The presence of FeSII is not only reflected by the respective peaks in the EPR spectrum (II_1 to II_3) but can also be inferred by the complex pattern of the FeSI signal. This shows a superposition of the split (I_{1a}, I_{1b}) and the unsplit (I_1) $\mathbf{g}_1$ components, a conclusion supported more clearly by data taken at even lower temperatures, i.e., 15 K instead of 30 K (Figure 3d). The unsplit component arises from a population of molecules in which the FeSI center is reduced while the FeSII center remains in the oxidized, diamagnetic state. The split one stems from molecules with both FeS centers in their reduced, paramagnetic states so that the dipolar interaction is visible. In addition, the $\mathbf{g}_2$ component of very rapid i becomes clearly split (marked by the sticks in Figure 3d), the temperature-dependent interaction amounts to approximately 0.7 mT for $\mathbf{g}_2$, which is in accordance with the parameters of Table 1. Figure 3e shows the spectrum of the fully reduced enzyme at 20 K; this, as in Figure 1e, shows only the iron sulfur species I and II. The splitting of FeSI is indicated by the arrows for comparison.

Rapid-freeze measurements were also conducted for the reaction of QuinOr and QualOx with their respective substrates. In Figure 4, curves a and b, the spectra obtained 10 ms after addition of quinoline (Quin, 2.5 mM) to QuinOr are shown at 80 and 30 K. By analogy with the IsoOr measurements, a very rapid species can be observed at 80 K, together with a FAD semiquinone signal. At lower temperatures, both these species are superimposed by the more anisotropic FeS signals. In spectrum 4b, a splitting of the very rapid signal of approximately 0.9 mT for $\mathbf{g}_2$ can be resolved (sticks), whereas the $\mathbf{g}_1$ and $\mathbf{g}_3$ features are masked by FeS signals. In contrast to the findings with IsoOr, the splitting cannot be ascribed unambiguously to the interaction with FeSI, because both FeS centers are reduced. On the other hand, the observed splitting is strikingly similar to that seen in the rapid-freeze spectra of IsoOr (Figure 1c). Traces c−e in Figure 4 show rapid-freeze spectra (10 ms) obtained for QualOx with the substrates quinaldine (Qual, traces c

Table 1: Parameters Used for the Simulation of the Interaction between Mo(V) and Iron−Sulfur Signals in IsoOr and QuinOr

spectrum	signal				
Figure 1d	IsoOr very rapid i	**g** tensor	2.0242	1.9550	1.9411
	30 K	line width (mT)	0.3	0.3	0.3
		D tensor (mT)	0.35	0.7	0.35
	IsoOr FeSI	**g** tensor	2.004	1.943	1.914
	30 K	line width (mT)	1.6	1.4	1.6
		D tensor (mT)	0.35	0.7	0.35
Figure 5b	QuinOr slow q	**g** tensor	1.967	1.966	1.958
	in H_2O, 70 K	**A** tensor (^1H) (mT)	1.65	1.7	1.5
		line width (mT)	0.4	0.4	0.5
Figure 5d	QuinOr slow q	***g*** tensor	1.967	1.966	1.958
	In H_2O, 35 K	**A** tensor (^1H) (mT)	1.65	1.7	1.5
		line width (mT)	0.35	0.35	0.4
		D tensor (mT)	0.5	0.5	1.0
		asymmetry parameter *E* (mT)	0.15		
Figure 5f	QuinOr slow q	**g** tensor	1.967	1.966	1.958
	in D_2O, 35 K	**A** tensor (^2H) (mT)	0.28	0.28	0.2
		line width (mT)	0.28	0.28	0.4
		D tensor (mT)	0.5	0.5	1.0
		asymmetry parameter *E* (mT)	0.15		

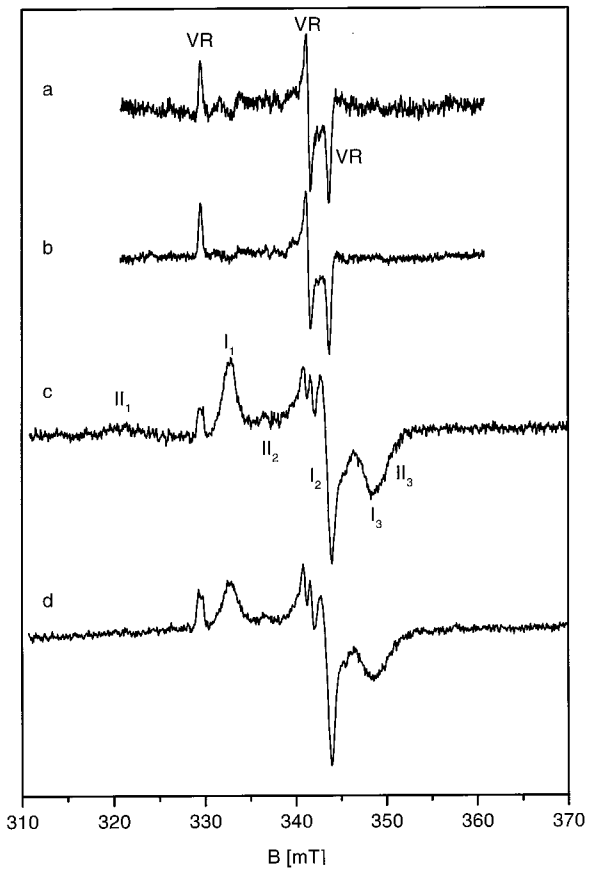

FIGURE 2: Rapid-freeze spectra of IsoOr obtained 10 ms after reaction with isoquinoline under different conditions showing the very rapid i and unsplit FeSI species: (a, c) addition of isoquinoline (45 μM) and potassium ferricyanide (1 mM) as artificial electron acceptor, (b, d) addition of isoquinoline (45 μM) in the absence of any final electron acceptor. Spectra a and b were recorded at 80 K, c and d at 30 K, the modulation amplitude was 0.5 mT (VR, molybdenum very rapid i; I, FeSI center; II, FeSII center).

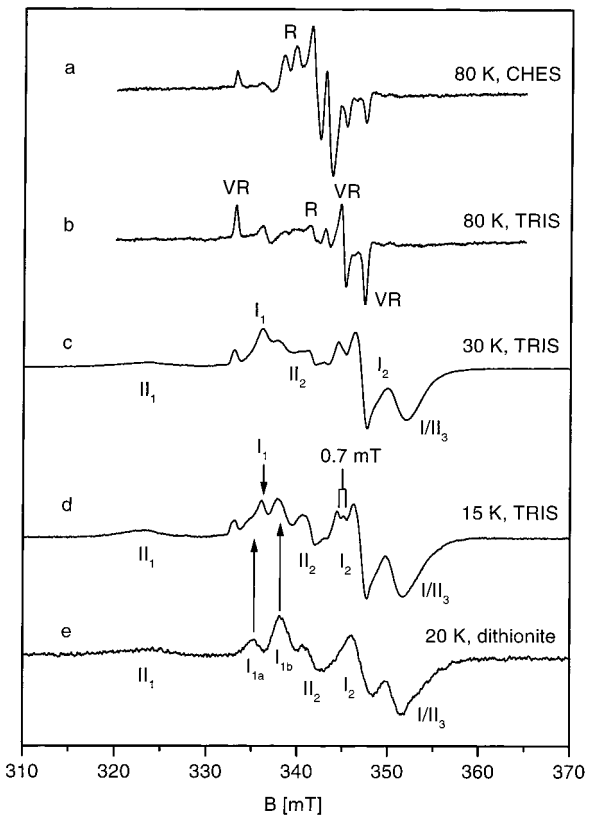

FIGURE 3: Spectra of IsoOr incubated for four minutes under manual freeze conditions with isoquinoline (2.5 mM) and without an artificial electron acceptor. (a, b) 80 K spectra at different pH values (a, pH 10, Ches buffer; b, pH 8, Tris-HCl buffer) showing the molybdenum signals rapid i and very rapid i in different proportions. (c, d) Low-temperature spectra of the sample incubated in Tris buffer exhibiting the splitting of the very rapid signal (marked by sticks) and contributions of split (I_{1a},I_{1b}) and unsplit FeSI species (I_1). (e) EPR spectrum (20 K) of a dithionite reduced IsoOr sample shown for comparison. The arrows indicate the positions of the split components in spectrum d. (R, molybdenum rapid i; VR, molybdenum very rapid i; I, FeSI center; II, FeSII center).

and d) and isoquinoline (Isoquin, trace e). Some differences from the analogous spectra of IsoOr and QuinOr are noteworthy. First of all, the very rapid species cannot be observed in the sample reduced with isoquinoline (trace e), whereas it can in the one reduced with quinaldine (traces c and d). This observation suggests different kinetic parameters of the QualOx turnover depending on the choice of the substrate. At lower temperatures, both samples show clear FeSII signals, but only traces of FeSI, whereas in the IsoOr rapid-freeze spectra FeSI is the dominant species. The third difference from the 30 K spectra of IsoOr and QuinOr is

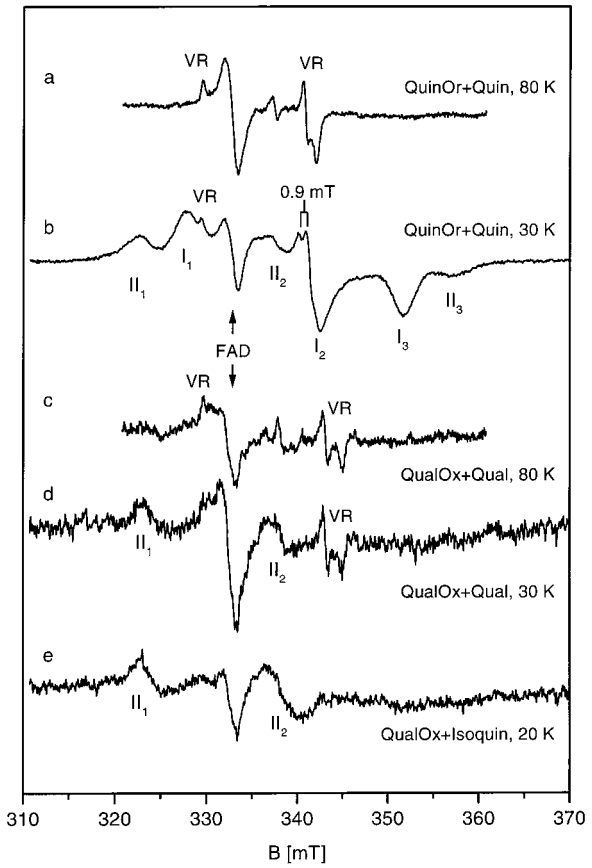

FIGURE 4: Rapid-freeze spectra of QuinOr and QualOx obtained 10 ms after reaction with different substrates (a and b, QuinOr + quinoline; c and d, QualOx + quinaldine; e, QualOx + isoquinoline; all 2.5 mM in Ches, pH 10). (a,b) Spectra of QuinOr showing the contributions of all reduced centers (FeSI, FeSII, FAD, very rapid) including a splitting of the $\mathbf{g}_2$-component of very rapid (sticks). (c−e) Spectra of QualOx showing signals of very rapid, FAD and FeSII. In contrast to QuinOr and IsoOr, the very rapid species is unsplit and does not appear in the isoquinoline reduced sample. Of the two FeS centers only the FeSII signal is present. (VR, molybdenum very rapid; I, FeS I center; II, FeS II center).

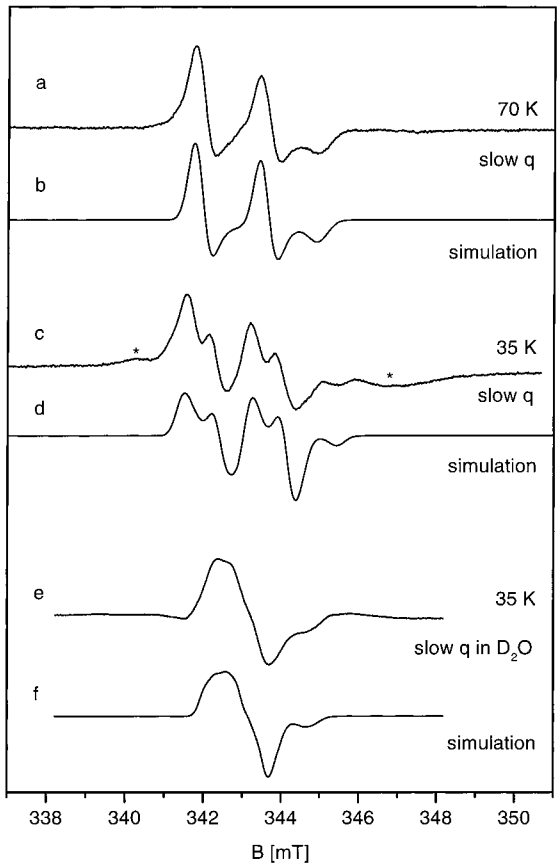

FIGURE 5: EPR spectra of cyanide-treated desulfo-QuinOr after reduction with sodium dithionite [slow Mo(V) signal]. Spectrum a shows the slow species with its characteristic proton coupling. In spectrum c, the same sample is cooled to 35 K, producing a splitting of the slow signal which is attributable to the interaction with iron−sulfur. Contributions of the iron−sulfur signals are marked by asterisks. Spectra b and d are the corresponding simulations of spectra a and c with parameters of Table 1. Spectrum e shows the slow species after D_2O exchange together with a simulation given in spectrum f. In all experimental spectra, small contributions of the rapid species were eliminated by subtraction.

the lack of a very rapid splitting (spectrum d). The signal remains unsplit even at 30 K.

A magnetic interaction monitored at the molybdenum in QuinOr was also seen for the so-called "slow q" signal prepared by addition of cyanide to the native enzyme and subsequent reduction with dithionite. In Figure 5, the spectrum of the slow q signal at 70 K (trace a) and its simulation (trace b) is shown. The signal is nearly axial with a proton splitting from a hydroxy group at the molybdenum center (*14*, *15*). Upon decreasing the temperature (to 35 K, trace c) a splitting becomes visible. This feature could be simulated (trace d) by introducing a **D** tensor with the parameters of Table 1, analogous to the very rapid i splitting of IsoOr. Again, **D** is assumed to be coaxial to the **g** tensor of the slow q signal and has its maximal component of 1 mT along $\mathbf{g}_3$. The spectrum also reveals the splitting caused by the smaller components (0.5 mT) of the **D** tensor along $\mathbf{g}_1$ and $\mathbf{g}_2$. To simulate these features, it proved necessary to introduce a small asymmetry parameter *E* of approximately 0.15 mT. In Figure 5e, the slow q spectrum obtained after proton exchange in D_2O is shown. The spectral features are less resolved since the hyperfine splitting of the ^2H atoms are of the same magnitude as the intrinsic line width of the slow q signal. A simulation was carried out (Figure 5f) by adopting the **D** tensor parameters from the spectra above and adjusting the natural line width and the ^2H hyperfine parameters. From these spectra, however, it cannot be decided which iron−sulfur species causes the splitting of the slow q signal, since both FeS signals are developed at 35 K (not shown).

Functionality of the IsoOr Sample and Kinetic Studies by Rapid-Freeze and Stopped-Flow Measurements. Before turning to a more detailed consideration of the kinetics using IsoOr, we consider the question of its functionality. Enzymes of the xanthine oxidase family are often contaminated with the nonfunctional desulfo-form and sometimes also with the de-molybdo form. For milk xanthine oxidase, the proportion of functional molecules may routinely be estimated (*24*) by comparing the A_{450} decrease elicited by brief exposure to the substrate with that obtained with dithionite. The persistence of the very rapid signal indicates, however, the incompleteness of reduction of functional IsoOr by the substrate. Although such a procedure is therefore scarcely likely to be valid for estimating the functionality of IsoOr, we nevertheless examined the sample used for rapid-freeze and stopped-flow experiments. The spectrum at pH 10.0 (250

mM Na^+-Ches; 1 mM EDTA) was similar to that reported in ref *19*. However, whereas the extent of bleaching by dithionite ($\Delta A_{470nm} = 9.0\ mM^{-1}\ cm^{-1}$) was in full agreement with these workers, bleaching by isoquinoline (1.4 mM) was considerably less extensive. Furthermore, there were significant absorbance changes in the time range 2−20 min after the additions. From the spectra recorded initially, the magnitude of the absorbance decrease at 450 nm with isoquinoline was 55% of that observed with dithionite. This may be taken as a lower limit for the percent functionality. This limit was raised by consideration of results of manual-mix EPR experiments in which the FeSI signal intensity with isoquinoline was 70−75% of that with dithionite, although it is again uncertain whether the substrate had fully reduced the FeS of the functional enzyme. For calculation purposes, as discussed below, a value of 80% functionality of this sample was therefore rather arbitrarily assumed. The activity of this IsoOr sample, assayed at pH 10.0 with isoquinoline and ferricyanide (see Materials and Methods), yielded a catalytic center activity of 5.4 ± 0.4 s^{-1} (per $2e^-$), corresponding to a corrected[2] functional enzyme catalytic center activity of 6.8 s^{-1}. Though systematic measurements of K_m values were not attempted, nevertheless, inspection of assay progress curves at different substrate concentrations suggested values ∼0.2 μM for isoquinoline and ∼0.1 mM for ferricyanide.

As mentioned before, IsoOr produces a long-lasting very rapid signal after addition of substrate (*15*). Since IsoOr is inhibited by isoquinoline on approximately the same timescale (*19*), it was hypothesized that the very rapid i species is associated with an inhibited state of the enzyme, comparable to the stable complex of xanthine oxidase with alloxanthine, which produces **g**-factors similar to the very rapid i signal (*25*). However, the rapid-freeze measurements reported here have shown that IsoOr behaves dramatically differently if an artificial electron acceptor is added. In the presence of potassium ferricyanide, the very rapid i signal has nearly completely vanished after 2 s reaction time (Figure 1, spectrum b). To provide information on the kinetics of IsoOr turnover in the presence of an artificial acceptor, the intensities obtained by integration of the very rapid i, FeSI, and FeSII signals were monitored on samples frozen in the time range 9 ms to 2 s. The results are shown as the experimental points in Figure 6b. It can be seen that all three signals remain developed up to about 220 ms and vanish in the period between 220 ms and 2 s. Parallel experiments at 9 ms reaction time but without ferricyanide gave data similar to those with ferricyanide.

To obtain additional kinetic information on the enzyme mechanism, we carried out stopped-flow experiments on IsoOr at room temperature analogous to the rapid-freeze studies described above. Absorption at 470 nm was followed during brief turnover of the enzyme by limiting amounts of isoquinoline in the presence of excess ferricyanide. Results at two different isoquinoline concentrations are presented in Figure 6a. These show a rapid decrease in A_{470nm}, followed by a relatively constant steady-state phase, the duration of which increased as the substrate concentration was increased,

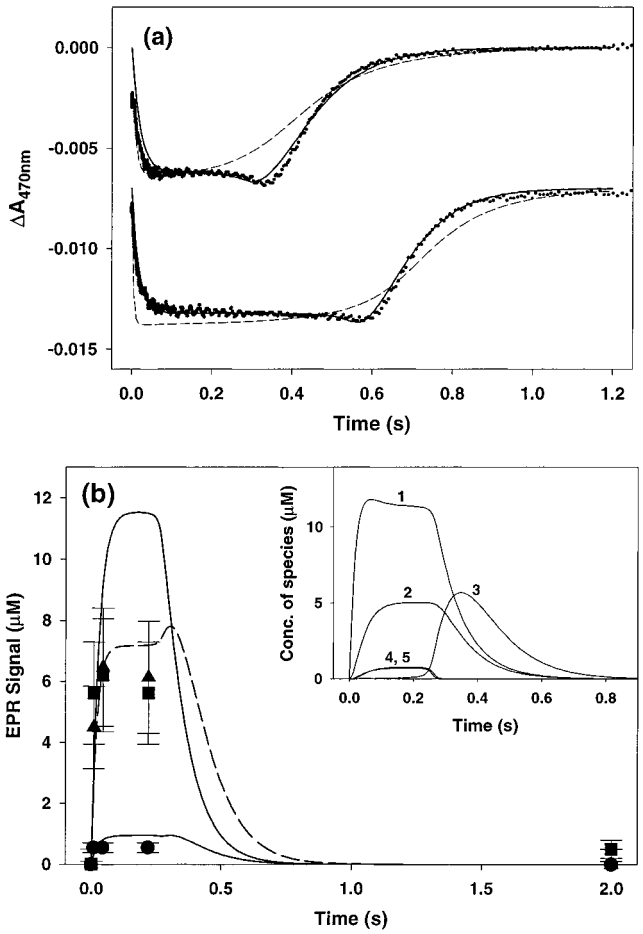

FIGURE 6: Time-course of absorbance changes and EPR signal intensities during brief turnover of IsoOr in the presence of ferricyanide. (a) shows stopped-flow traces recorded at 470 nm and (b) intensities of the different EPR signals followed by rapid freezing. Functional enzyme and substrate concentrations (μM) after mixing were, respectively, (a) (upper traces) 3.05 and 7.55, (lower traces) 3.05, 15.1; (b) 18.0, 45.0. Ferricyanide (1 mM) was present in all experiments and reaction was initiated by mixing enzyme from one syringe of the apparatus with isoquinoline and ferricyanide from the other. All curves through the experimental data points were calculated from Scheme 3 with a single set of parameters, with the exception of the broken lines in (a) which were calculated from Scheme 1. Symbols in panel b are as follows: very rapid Mo(V), squares; FeSI, triangles; FeSII, circles; the corresponding calculated curves are shown: *continuous*, *broken* and *continuous*, respectively. The inset panel in panel b shows the calculated concentrations for this experiment of the species of Scheme 3: curve 1, E(2e)-P; curve 2, E(1e)-P; curve 3 E(1e); curves 4 and 5 (virtually superimposed), E(1e)-S and E(3e)-P. Experiments were at pH 10.0 in 250 mM Na^+-Ches at 21 °C, except for panels a (upper traces) which was at about 19 °C. Rate constants for the Scheme 1 simulations were as follows: k_{+1} 2.00 × 10^7 M^{-1} s^{-1}, k_{-1} 4.0 s^{-1}, k_{+2} 2000 s^{-1}, k_{+3} 7.0 s^{-1}; absorbance scaling was arbitrary. For the Scheme 3 simulations, rate constants were as follows: k_{+1} 4.3 × 10^8 M^{-1} s^{-1}, k_{-1} 0.0 s^{-1}, k_{+2} 45 s^{-1}, k_{+3} 13.2 s^{-1}, k_{+4} 31 s^{-1}, k_{+5} 2.0 × 10^8 $M^{-1}s^{-1}$, k_{-5} 1.0 s^{-1}, k_{+6} 210 s^{-1}, k_{+7} 195 s^{-1}, k_{+8} 15.5 s^{-1}; the absolute magnitudes of the absorbance changes were simulated as described in the text. With both schemes, for the experiment at 19 °C, all rate constants were reduced by a factor of 1.145. Note that in panel a (lower traces) zero absorbance change is offset to −0.007.

followed finally by a relatively slow return to the initial A_{470nm} value. A noteworthy feature of the traces is the "overshoot" in the form of a small A_{470nm} decrease as the end of the steady-state was neared. This was observed consistently in a considerable number of experiments in addition to those

[2] The value assumed for the percentage functionality affects not only the corrected catalytic center activity but is also relevant to the values of parameters in the kinetic simulations. See also footnote number 4.

Scheme 1: Model of the Mechanism of IsoOr Turnover in the Presence of Ferricyanide[a]

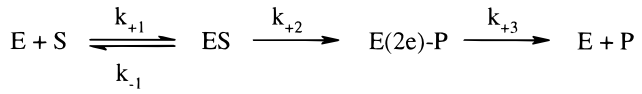

[a] E, enzyme; S, substrate; P, product (1-hydroxy-isoquinoline); ES, corresponding Michaelis−Menten complex; E(2e)-P, species formed after transfer of two electrons from the substrate to the enzyme, detectable by the very rapid i signal.

illustrated. The magnitude of the steady-state decrease in A_{470nm} of about 0.006 (Figure 6a) corresponds to only 22% of the decrease that would be expected for full reduction by dithionite of this concentration of functional enzyme (with $\Delta\epsilon = 9\ mM^{-1}\ cm^{-1}$).

DISCUSSION

Rapid-Freeze EPR Data. The analysis of the reaction of IsoOr with isoquinoline with and without an artificial electron acceptor has demonstrated that the unusual longevity of the very rapid i species (*15*) is due to the absence of a natural electron acceptor. The kinetics of IsoOr turnover as observed in the rapid-freeze experiments suggest Scheme 1.

According to this scheme, the enzyme reacts with the substrate in a 2e-reaction to yield E(2e)-P, the species giving rise to the very rapid i signal, which is decomposed by ferricyanide to the enzyme and the product, with no intermediates detected. The data suggest that the last step of the kinetic scheme, the decomposition of the product-bound, reduced enzyme species E(2e)-P is rate limiting, so that most of the enzyme is present as E(2e)-P throughout the time range for which signals were observed during the turnover experiment. At the concentrations of functional enzyme and substrate used in Figure 6b, 2.5 turnovers would be required to exhaust the substrate. On the basis of the catalytic center activity of the functional enzyme measured under identical conditions (see Materials and Methods) of 6.8 s^{-1}, substrate exhaustion would be expected after 290 ms, a value consistent with the data. Thus, in the presence of ferricyanide the very rapid i species behaves as a catalytically competent intermediate, comparable to the very rapid species of xanthine oxidase. This finding, together with the similarity of the EPR signals of FeS-centers and Mo(V)-species as well as a 30−40% identity in amino acid sequence to other related enzymes (*26*), imply that the very similar structural properties and the common reaction mechanism of the xanthine oxidase family also apply to IsoOr.

Manual-Mixing EPR Data. In the absence of an added oxidant, however, IsoOr shows a behavior which is drastically different from that of the related enzymes XanOx and QuinOr. Apart from the longevity of the very rapid i species, the experimental spectra obtained under manual freeze conditions show a significant development of the reduced FeSII signal and the rapid Mo(V) species (*15*). These observations may now be explained by Scheme 2. It proposes a model for the IsoOr reactions in the absence of an artificial acceptor which is, up to the point of the formation of E(2e)-P, identical to Scheme 1. Due to the lack of a final electron acceptor, the complex E(2e)-P is obviously not reoxidized. We propose that this species decays spontaneously byproduct release to yield E(2e), a two-electron-reduced enzyme species and the product, as does the corresponding species from xanthine oxidase or quinoline oxidoreductase. This, however, occurs on a much longer time scale, so that the very rapid i species can be monitored under manual freeze conditions. Using an excess of substrate as in the manual freeze experiments, the species E(2e) reacts rapidly with excess substrate to form E(2e)-S, the substrate-binding reduced enzyme species, which produces the rapid signal and the fully reduced enzyme state E(4e). At pH 10, conditions are clearly more favorable for the formation of the rapid species than at pH 8.

Scheme 2: Model of the Enzymatic Action of IsoOr in the Absence of an Electron Acceptor[a]

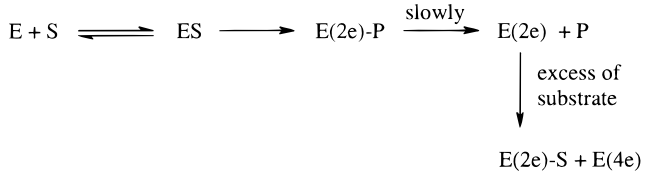

[a] The product-bound species E(2e)-P decays slowly thus enabling the associated very rapid signal to be stable for a prolonged time. With excess substrate the reduced enzyme may take up two additional electrons or react with substrate molecules to form the rapid species. (Note that species with odd numbers of electrons, produced by disproportionation reactions or by reaction with the desulfo enzyme may also be involved)

In E(2e)-P, the two electrons are statistically distributed among the three centers, yielding the very rapid FeSI and FeSII signals as well as an EPR-silent Mo(IV) form. The splittings observed in the EPR spectra give important indications of the redox state of neighboring centers. The very rapid signal is split when the second electron is on FeSI, and FeSI is split when the second electron is on FeSII. In the experimental spectra obtained by rapid-freeze, only split very rapid and unsplit FeSI signals are observed, together with traces of FeSII. This shows that the main species has FeSI reduced and Mo(V) present. The predominance of the FeSI is consistent with its higher redox potential compared to the redox potential of FeSII [$E_{FeSI} = 65$ mV, $E_{FeSII} = 10$ mV (*15*)].

According to Scheme 2, the spectra after about 4 min reaction time should consist of the species E(2e)-S and E(4e), together with contributions from E(2e)-P and E(2e). Significantly, spectra recorded at this reaction time show the reduced FeSII center, together with a split FeSI signal. This observation implies that the species appearing later in the enzymatic cycle, i.e., E(2e), E(2e)-S, and E(4e) contain a higher proportion of the state having both FeS centers reduced than the species E(2e)-P.

Stopped-Flow Data and Quantitative Kinetic Interpretation. Satisfactory simulations (not shown) could be obtained of the time course of very rapid signal intensity (cf. caption of Figure 6b) based in Scheme 1, using a value k_{+3} consistent with the observed catalytic center activity and with k_{-1}/k_{+1} consistent with K_m. However, this scheme had to be extended in order to explain the stopped-flow data. This is clear from the simulations illustrated as dashed lines through the data points in Figure 6a. In simulations based on this scheme, it was found that whatever values of the rate constants were employed, the predicted A_{470} tended to increase rather than to decrease during the steady-state period, with no sign whatever of the observed "overshoot" at its end. A more complex scheme is therefore clearly required.

Scheme 3: Elaboration of Scheme 1 Required to Account for Stopped-Flow Data on Enzyme Turnover[a]

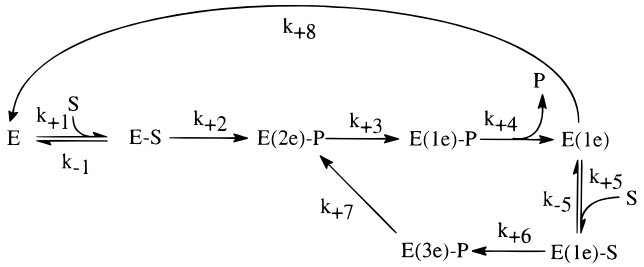

[a] Separate reaction steps with two ferricyanide molecules are involved. P dissociates following reaction with the first of these; k_{+3}, k_{+7}, and k_{+8} all correspond to reaction with ferricyanide. All reduced species will contribute to the FeS signals and A_{470} decreases; E(1e)-P, E(2e)-P, and E(3e)-P will contribute to the very rapid signal.

The most obvious oversimplification in Scheme 1 is that reaction with ferricyanide is shown as a single reaction step, whereas in reality, the reaction of two successive ferricyanide molecules must be involved. Particularly, if the reaction with ferricyanide is indeed rate limiting, then resolving it into two steps opens the possibility of E(1e)-P produced in the first step, undergoing further transformations before reacting with the second ferricyanide. This is illustrated in Scheme 3, according to which, governed by k_{+4}, bound product dissociates from E(1e)-P, yielding E(1e). This in turn can then react either (k_{+8}) directly with the second ferricyanide molecule, or alternatively, bearing in mind the low value of K_m, it can react (k_{+5}) with a further substrate molecule, thus entering into an alternative catalytic cycle (governed by k_{+5}, k_{+6}, k_{+7}, k_{+3}, k_{+4}, in contrast to the primary cycle, governed by k_{+1}, k_{+2}, k_{+3}, k_{+4}, k_{+8}). That such a scheme might, with appropriate values of the rate constants, be capable of accounting for the observed overshoot, is suggested by consideration of the likely distribution of electrons among the three redox centers in the different reduced enzyme species. Olson et al. (*27*) introduced the concept of the oxidized substrate molecule binding tightly to the reduced states of the molybdenum atom of xanthine oxidase, thereby greatly stabilizing such enzyme forms. Thus, the redox potentials of molybdenum bearing a covalently bound intermediate, as in the species E(1e)-P, E(2e)-P, and E(3e)-P, are predicted to be much higher than those in the remaining species of Scheme 3. It follows that while in E(1e)-P the electron is expected to be mainly on Mo, for E(1e) it will be mainly on FeS. Hence, as substrate becomes exhausted, the level of E(1e) will transiently be enhanced, leading to additional reduction of FeS centers and thus, potentially, accounting for the observed overshoot.

Optimized simulations of the stopped-flow data bear out the validity of the above prediction. Not only the form of the time course at the two substrate concentrations used but also the magnitude of the observed ΔA_{470} values were successfully simulated (Figure 6a, continuous lines), as follows. To calculate the absorbance changes, it is necessary not only to predict the time course for each of the species of Scheme 3 but also to know for each the difference between its molar absorption coefficient and that of the resting oxidized enzyme. The distribution of electrons among the different redox centers in the various reduced IsoOr species were calculated (Table 2) on the assumption (*27*) of rapid equilibrium and a statistical distribution of the electrons

Table 2: Calculated Electron Distributions in the Different IsoOr Reduced Species of Scheme 3[a]

fraction	E(2e)-P	E(1e)-P	E(1e), E(1e)-S	E(3e)-P
Mo(VI)	0.0002	0.0043	1.000	0.0000
Mo(V)	0.566	0.996	0.000	0.112
Mo(IV)	0.433	0.000	0.000	0.888
$FeSI_{red}$	0.505	0.004	0.892	0.904
$FeSII_{red}$	0.061	0.000	0.108	0.208

[a] The values listed are those that were used in the kinetic simulations illustrated in Figure 6. Calculations were performed as described in ref *27*, based on a redox potential-controlled statistical distribution of the electrons. For all species the following measured (*15*) redox potentials of the FeS centers were used: FeS I +65 mV, FeSII +10 mV. For species without bound product a value of −240 mV was assumed for the Mo(VI)/Mo(V) and Mo(V)/Mo(IV) potentials. For species with bound product the following potentials were used: Mo(VI)/Mo(V), +210 mV; Mo(V)/Mo(IV), +61 mV (see also footnote 3).

controlled by the redox potentials of the individual centers. For these calculations, the FeSI and FeSII potentials of +65 and +10 mV (*15*) were employed. Potentials relating to the molybdenum are, however, not available from EPR-detected potentiometric titrations and had to be estimated or evaluated from the data. The values assumed for the Mo(VI)/Mo(V) and the Mo(V)/Mo(IV) potentials of the free enzyme species and for the Mo(VI)/Mo(V) potential of species with bound product, are listed in Table 2. Calculated electron distributions were found to be quite insensitive to the exact value of any of these three molybdenum potentials.[3] The last potential, that for Mo(V)/Mo(IV) in the product-bound species, was varied (see Materials and Methods), along with all the rate constants in Scheme 3 until the optimized fits illustrated in Figure 6a were obtained, yielding the final value (Table 2) of +61 mV.

In calculating the absorbance changes from the electron distributions of Table 2, the assumption was made that FeSI and FeSII contribute equally and Mo negligibly, with full reduction of the enzyme corresponding to $\Delta\epsilon_{470nm} = 9\ mM^{-1}\ cm^{-1}$. Thus, the molar absorption coefficient changes were calculated for each species and the absorbance change at each time was then obtained by summing for each species present, the product of its concentration and its $\Delta\epsilon_{470nm}$.

The good agreement of ΔA_{470} time course calculated as above with the experimental results in Figure 6a provides considerable support for the validity of the mechanism of Scheme 3. In Figure 6b, the rapid-freeze EPR data are compared with the corresponding simulations, based on the same scheme and the same values of all the parameters. In the inset panel, the calculated time course for each reduced

[3] For both the Mo(VI)/Mo(V) and the Mo(V)/Mo(IV) potentials in the free enzyme species a value of −240 mV (Table 2) was used in the calculations, which is within the range of values observed for these potentials in enzymes of the xanthine oxidase family. This corresponds to essentially no reduction of Mo in the E(1e) and E(1e)-S species. However, the calculated electron distributions as listed in Table 2 are unchanged for any value of these potentials below −140 mV. Above this value small amounts of Mo(V) appear in these species, with a corresponding decrease in the amount of $FeSI_{red}$. Molybdenum potentials for the product-bound species were arbitrarily varied until the desired electron distributions were achieved. These were found to be much less sensitive to the value chosen for Mo(VI)/Mo(V) than to that for Mo(V)/Mo(IV). A high value for the former ensures that in E(1e)-P, the single electron is largely located on Mo. Accordingly, the former potential was fixed, at the value indicated, at an earlier stage in the fitting procedure than the latter.

species is shown. The transient accumulation of E(1e) at the end of the steady-state is noteworthy. As predicted, it is this accumulation that is responsible for the overshoot in the stopped-flow data. Though the time course of the EPR signals, predicted in the above manner from the stopped-flow, is consistent with the simulations (Figure 6b), as are the absolute intensities of the FeSI signals, the FeSII signals are rather weaker than predicted and the very rapid signals are of only about half the predicted intensity. However, this may be taken as satisfactory agreement with the scheme, bearing in mind the rather arbitrary nature of some of the assumptions that have been made, especially in relation to the percent functionality of the enzyme. Consideration of the rate constants used in the simulations (Figure 6 caption) implies that under steady-state conditions the two catalytic cycles will proceed side-by-side but with the E(1e)/E(3e) cycle running slightly faster than the E/E(2e) cycle. Conversely, Table 2 shows that the ratio of steady-state intensities FeSI and very rapid signals will be extremely sensitive to any change in the relative amounts of E(1e)-P and E(2e)-P. Thus, the predicted relative steady-state EPR signal intensities will be highly sensitive to small changes in the relative rates of the two cycles. The overall quality of the simulation was further tested by calculating, with the same values of the rate constants, the predicted rate of product appearance in the presence of excess substrate. The value obtained was 8.4 s^{-1}, in reasonable agreement with the observed enzyme catalytic center activity of 6.8 s^{-1}. Overall, the data thus strongly support the applicability of the mechanism of Scheme 3 to the action of IsoOr. Though no great precision is claimed for the numerical interpretations, it seems likely that the values of all the parameters used in the simulations are at least of the correct order of magnitude.[4] The low K_m values indicated by k_{-1}/k_{+1} and k_{-5}/k_{+5} are noteworthy.

In the context of the redox potentials of the FeS centers used in the above simulations, caution might have been needed since the values were obtained under nonturnover conditions and at a different pH value from the rapid-freeze spectra (*15*). However, their relevance is emphasized by the observation that the QualOx rapid-freeze spectra show only the FeSII signal without traces of FeSI, in contrast to the situation in IsoOr. This is consistent with the reversed order of the redox potentials in QualOx ($E_{FeSI} = -250$ mV, $E_{FeSII} = -70$ mV). Additionally, for QuinOr, the EPR spectra (30 K) obtained under rapid-freeze conditions show a lower relative intensity of the FeSII signal in comparison to the manually frozen sample reduced with an excess of dithionite. This indicates a lower degree of reduction of the FeSII center in redox equilibrium, which is again consistent with the measured potentials of QuinOr ($E_{FeSI} = -155$ mV, $E_{FeSII} = -195$ mV). As expected (*28*), a reaction time of 10 ms is sufficiently long enough to generate an equilibrium between the FeS centers, which leads to the exclusive reduction of the FeSII center.

In terms of redox potentials and calculated electron distributions, rates of decay of the product-bound species of IsoOr, E(1e)-P, E(2e)-P, and E(3e)-P might be predicted to be proportional to, or related to, the fraction of molybdenum in each in the Mo(VI) state. Thus, according to Table 2, E(1e)-P with 0.43% of its molybdenum as Mo(VI) is indeed expected to be the fastest decaying of the three species, with E(2e)-P at 0.02%, substantially behind it.[5]

Mechanism of Substrate Oxidation at the Molybdenum Center. The unusual behavior of the very rapid i signal (longevity in the absence and rapid decay in the presence of an oxidizing acceptor) is interesting with respect to the mechanism of xanthine oxidase action. There are two mechanisms currently under discussion. The first one (*11*, *17*, 29) is based on a nucleophilic attack on the C-8 atom of xanthine by a deprotonated water ligand of the molybdenum center followed by hydride transfer from the resulting tetrahedral intermediate to the sulfido ligand. This results in a Mo(IV) species which converts to the very rapid intermediate after electron transfer to the FeS centers. The signal-giving species contains the product σ-bonded via the oxygen atom of the hydroxy-group. The second mechanism (*18*, *30*, *31*) postulates the addition of the C-8—H bond of xanthine across the Mo=S bond to give a Mo(VI) species with a Mo—C bond. The deprotonated water ligand of Mo subsequently attacks to give a side-on bound Mo(IV) carbonyl species which converts to the very rapid intermediate by electron transfer to the FeS centers. Lowe and co-workers (*18*) have pointed out that stable versions of such side-on bound carbonyl species involve lower valence molybdenum centers. At the Mo(V) state, the proposed side-on interaction can only involve a single electron and therefore must be very weak; at the Mo(VI) stage no back-bonding interaction is possible, so the product leaves. Thus, the second mechanism accounts very simply for the observation of a fast decay of the very rapid i species of IsoOr, with product loss, on oxidation of Mo to Mo(VI). Conversely, the first mechanism provides no explanation for this phenomenon.

Indeed, on the contrary, recent theoretical work by Voityuk and co-workers (*32*) implies that, according to the first mechanism, the product should dissociate freely from the enzyme in the Mo(IV) state. These workers performed calculations in relation to the oxidation of formaldehyde by

[4] The assumption of 80% functionality for the enzyme has a bearing on the values of the parameters. Indeed, with further computing this value might have been floated and a still better fit obtained, though the precision of the data would limit the usefulness of such an exercise. Qualitatively, some indication of the effect of varying this parameter on the simulations may be given by the following considerations. If in reality the enzyme was 100% functional, then the observed steady-state absorbance changes would correspond to proportionately lower molar absorption coefficients changes. To simulate this, a small shift in the relative rates of the two catalytic cycles so as to favour E(1e)-P at the expense of E(2e)-P would be necessitated. Such a change would tend not only to increase the predicted very rapid signal intensities, giving a better fit to the data, but would also tend to reduce the predicted rate of product appearance, again tending to a better fit to the data.

[5] By analogy, such arguments may be extended to a comparison of IsoOr with XanOx. From the potentials for the latter assumed by Olson et al. (*27*), the Mo(VI) percentages for E(1e)-P and E(2e)-P may be calculated and are distinctly higher than for IsoOr, at 1.5% and 0.15%, respectively. Such differences of Mo(VI) percentages between the enzymes may seem rather small in comparison with the large observed very rapid signal stability differences, though they are in the expected direction. However, in the work of Olson et al. as well as in our work, the Mo(VI)/Mo(V) potential of product-bound species must have been difficult to establish precisely. Had this potential been overestimated by these workers by 40 mV, then the Mo(VI) values for E(1e)-P and E(2e)-P of X anOx would have become substantially larger, at 6.5% and 0.68%, respectively (with only very small accompanying other changes in the electron distributions). Thus, the extrapolation from our data on IsoOr remains reasonable, that in both enzymes, product dissociates only from those molecules in which Mo is in the Mo(VI) state.

xanthine oxidase family enzymes, interpreting their results in terms of the first mechanism. An important conclusion was that the product, in this case formic acid, was rather weakly bound to the reduced molybdenum center, thus, permitting its facile replacement by a water molecule with molybdenum remaining as Mo(IV). It is generally assumed that all xanthine oxidase family enzymes act on all substrates by a common reaction mechanism. Our data show conclusively that the product of IsoOr action, 2H-1-oxo-isoquinoline, does not dissociate from the Mo(V) state of this enzyme, at least within 1 h, and that in all probability, it dissociates only from those enzyme molecules in which the metal is in the Mo(VI) state. The work of Voityuk et al. (*32*) therefore further strengthens the conclusion from our work favoring the second reaction mechanism over the first.[6]

Identity of the FeSI and FeSII EPR Signal-Giving Species. The splitting of the very rapid i signal under rapid-freeze conditions sheds some light on the question as to which of the two FeS clusters is close to the molybdopterin cofactor. This question arose after the determination of the crystal structure of aldehyde oxidoreductase (*12, 13*), which shows that one of the FeS centers is bridged by hydrogen bonding to the pterin ring with an Mo−Fe distance of ca. 15 Å and is buried inside the protein. This "proximal" FeS-center possesses a unique fold, a four helix bundle with two longer, central helices flanked by two shorter peripheral ones. The other "distal" FeS center exhibits a fold typical for plant-type ferredoxins and is located close to the surface of the domain with solvent contacts at distances of 24.6 Å from the molybdenum ion and 12.3 Å from the closest iron atom of the proximal FeS center. It has been suggested that for XanOx, FeSI is proximal to the Mo(V) center, based on analysis of dipolar interactions, temperature dependence, and saturation behavior of EPR signals, although minor different estimates of distances were obtained (*34*−*36*). On the other hand, H−D exchange ENDOR experiments indicated FeSII to be buried inside the enzyme (*37*). Up to now it is not clear which of the clusters characterized by EPR (denoted I or II) should be associated with the FeS center neighboring the molybdopterin cofactor. In the case of IsoOr, the observed splitting must be interpreted as a magnetic interaction between the Mo(V) state and reduced FeSI, because FeSII is present only in traces in the spectra obtained after 10 ms. For QuinOr, this assignment is less clear, since in the spectra obtained under rapid-freeze conditions, both centers are reduced. However, the similarity of the splitting of the very rapid signals points at a similar arrangement of the interacting centers in IsoOr and QuinOr. For QualOx, low-temperature spectra of the species reduced with quinaldine show an unsplit very rapid signal. Due to the reverse order of the redox potentials of QualOx compared to QuinOr and IsoOr, these spectra exhibit only reduced FeSII centers, whereas FeSI remains oxidized. Thus, the absence of a splitting must be expected if it is assumed that for QualOx the FeSI cluster is also close to the molybdopterin cofactor. So far, these results confirm previous data from interaction studies with xanthine oxidase (*36*), in which an interaction of approximately 1.1 mT between Mo(V) signals and FeSI was observed. However, the magnitude of the interaction of IsoOr and QuinOr is smaller. The maximum coupling for both enzymes is always observed for the $\mathbf{g}_2$ component of the very rapid signal, and its magnitude varies between 0.7 mT for IsoOr and 0.9 mT for QuinOr. For the $\mathbf{g}_1$ or $\mathbf{g}_3$ components, the interaction is much smaller and can only be detected through line width effects. For the slow q signal of QuinOr, a maximal coupling of 1.0 mT along $\mathbf{g}_3$ was simulated. Obviously the $\mathbf{g}_2$ component of very rapid i and $\mathbf{g}_3$ of slow q point to the direction of maximal interaction, i.e., to the vector of the center-to-center distance. On the basis of a point−dipole approach, the values of 0.7 mT for IsoOr and 1.0 mT for QuinOr correspond to a distance of 17.2 and 15.3 Å, respectively, between FeSI and Mo.

Thus, we conclude that for IsoOr and by analogy for the enzymes QualOx and QuinOr, the FeSII signal comes from the "distal" iron−sulfur cluster that is remote from molybdenum and close to the surface of the molecule (*12*), whereas the "proximal" cluster which has the more unusual sequence motif in the AldOr structure gives the FeSI signal and is interacting with the molybdenum center of IsoOr and QuinOr.

[6] The calculations of Voityuk et al. (*32*) were not extended to Mo(V) species and in particular to a formaldehyde-derived very rapid species, no doubt because to our knowledge such a signal has never been observed from any xanthine oxidase family enzyme. In this connection, it would be particularly interesting in relation to the present work if the calculations were extended to formamide, which is both a good substrate of milk xanthine oxidase and gives a very rapid signal (*33*).

ACKNOWLEDGMENT

We wish to thank Ms. Sury and Ms. Krauss (University of Hohenheim) for their efforts in preparing numerous enzyme samples and Prof. R. L. Richards (John Innes Centre) for discussions.

REFERENCES

1. Bray, R. C., and Swann, J. C. (1972) *Struct. Bonding 11*, 107−144.
2. Bray, R. C. (1975) in *The Enzymes* (Boyer, P. D., Ed.) pp 300−419, Academic Press, New York.
3. Bray, R. C. (1980) *Adv. Enzymol. Relat. Areas Mol. Biol. 51*, 107−165.
4. Coughlan, M. (1980) in *Molybdenum and Molybdenum-containing Enzymes* (Coughlan, M., Ed.) pp 119−185, Pergamon Press Oxford.
5. Gutteridge, S., and Bray, R. C. (1980) in *Molybdenum and Molybdenum-containing Enzymes* (Coughlan, M., Ed.) pp 223−239, Pergamon Press, Oxford.
6. Cramer, S. P. (1983) in *Advances in Inorganic and Bioinorganic Mechanisms* (Sykes, A. G., Ed.) pp 259−315, Academic Press, London.
7. Hille, R., and Massey, V. (1985) in *Molybdenum Enzymes* (Spiro, T. G., Ed.) pp 443−517, J. Wiley and Sons, Inc., New York.
8. Bray, R. C. (1988) *Q. Rev. Biophys. 21*, 299−329.
9. Pilato, R. S., and Stiefel, E. I. (1993) in *Bioorganic Catalysis* (Reedijk, J., Ed.) pp 131−188, Marcel Dekker, Inc., New York.
10. Hille, R. (1994) *Biochim. Biophys. Acta 1184*, 143−169.
11. Hille, R. (1996) *Chem. Rev. 96*, 2757−2816.
12. Romao, M. J., Archer, M., Moura, I., Moura, J. J. G., LeGall, J., Engh, R., Schneider, M., Hof, P., and Huber, R. (1995) *Science 270*, 1170−1176.
13. Romao, M. J., and Huber, R. (1998) in *Metal Sites in Proteins and Models* (Hill, H. A. O., Sadler, P. J., Thomson, A. J., Eds.) pp 1−37, Springer, Berlin.
14. Tshisuaka, B., Kappl, R., Hüttermann, J., and Lingens, F. (1993) *Biochemistry 32*, 12928−12934.

15. Canne, C., Stephan, I., Finsterbusch, J., Lingens, F., Kappl, R., Fetzner, S., and Hüttermann, J. (1997) *Biochemistry 36*, 9780−9790.
16. Bray, R. C., and George, G. N. (1985) *Biochem. Soc. Trans. 13*, 560−567.
17. Hille, R. (1997) *J.Biol. Inorg. Chem. 2*, 804−809.
18. Lowe, D. J., Richards, R. L., and Bray, R. C. (1997) *Biochem. Soc. Trans. 25*, 774−778.
19. Lehmann, M., Tshisuaka, B., Fetzner, S., Röger, P., and Lingens, F. (1994) *J. Biol. Chem. 269*, 11254−11260.
20. Stephan, I., Tshisuaka, B., Fetzner, S., and Lingens, F. (1996) *Eur. J. Biochem. 236*, 155−162.
21. Bray, R. C. (1961) *Biochem. J. 81*, 189−193.
22. Gutteridge, S., Tanner, S. J. and Bray, R. C. (1978) *Biochem. J. 175*, 869−878.
23. Aasa, R., and Vänngård, T. (1975) *J. Magn. Reson. 19*, 308−315.
24. Morell, D. B. (1952) *Biochem. J. 51*, 657−666.
25. Hawkes, T. R., George, G. N., and Bray, R. C. (1984) *Biochem. J. 218*, 961−968.
26. Lehmann, M., Tshisuaka, B., Fetzner, S., and Lingens, F. (1995) *J. Biol. Chem. 270*, 14420−14429.
27. Olson, J. S., Ballou, D. P., Palmer, G. and Massey, V. (1974) *J. Biol. Chem. 249*, 4363−4382.
28. Hille, R., and Anderson, R. F.. (1991) *J. Biol. Chem. 266*, 5608−5615.
29. Huber, R., Hof, P., Duarte, R. O., Moura, J. J. G., Moura, I., Liu, M. Y., Legall, J., Hille, R., Archer, M., and Romao, M. J. (1996) *Proc. Natl. Acad. Sci. U.S.A. 93*, 8846−8851.
30. Howes, B. D., Bray, R. C., Richards, R. L., Turner, N. A., Bennett, B., and Lowe, D. J. (1996) *Biochemistry 35*, 3874−3874.
31. Lowe, D. J., Richards, R. L., and Bray, R. C. (1998) *J. Biol. Inorg. Chem. 3*, 557−558
32. Voityuk, A. A., Albert, K., Rõmao, M. J., Huber, R., and Rösch, N. (1998) *Inorg. Chem. 37*, 176−180.
33. Morpeth, F. F., George, G. N., and Bray, R. C. (1984) *Biochem. J. 220*, 235−242.
34. Bertrand, P., More, C., Guigliarelli, B., Fournel, A., Bennet, A., and Howes, B. (1994) *J. Am. Chem. Soc. 116*, 3078−3086.
35. Barber, M. J., Salerno, J. C., and Siegel, L. M. (1982) *Biochemistry 21*, 1648−1656.
36. Lowe, D. J., and Bray, R. C. (1978) *Biochem. J. 169*, 471−479.
37. Lowe, D. J., Mitchell, C. J. and Bray, R. C. (1997) *Biochem Soc. Trans. 25*, 527S.

BI991089S